

Research on Optimization Design Based on Heliostat Field

Wenbo Zuo^{1,*}, Ruoyu Wang², Bowen Xing²

¹Petroleum Institute, China University of Petroleum (Beijing) Karamay Campus, Xinjiang, Karamay 834000, China

²Engineering College, China University of Petroleum (Beijing) Karamay Campus, Xinjiang, Karamay 834000, China

*Corresponding author: 15939022324@163.com

Abstract: Heliostat field solar thermal power generation is an environmentally friendly technology that harnesses solar energy. It offers a clean and cost-effective method of generating power. Unlike some other solar technologies, it can provide uninterrupted energy day and night through efficient thermal storage systems, ensuring a stable and continuous power supply. This feature significantly enhances solar energy's effective utilization. The advantages of solar thermal power generation make it highly competitive in the commercial energy market. To optimize its design, this article calculates parameters such as annual average optical efficiency, output thermal power, and output thermal power per unit mirror area. It also considers constraints like heliostat size, layout, and collector placement to achieve a targeted annual average thermal power output of 60MW. By carefully adjusting the position coordinates of the absorption tower, heliostat size, installation height, the number of heliostats, and their positioning, an optimal solution is derived. The design strives to maximize the annual average output thermal power per unit mirror area while meeting specified criteria, ultimately improving the field's overall performance. This optimization aims to fully leverage solar energy resources, achieve maximum energy utilization, and economic benefits. In doing so, it contributes to sustainable development and green energy goals.

Keywords: Heliostat field, Utilization of solar energy resources, Unit mirror area, Output thermal power

1. Introduction

Building a new type of power system with new energy as the main body is an important measure for China to achieve the goals of "carbon peaking" and "carbon neutrality". Tower solar thermal power generation ^[1] is a low-carbon and environmentally friendly new clean energy technology. The heliostat is the basic component of a tower solar thermal power station (hereinafter referred to as a tower power station) that collects solar energy. Its base is composed of a longitudinal and a horizontal rotating shaft, and the flat reflector is installed on the horizontal rotating shaft. The axis of the longitudinal axis is perpendicular to the ground, which can control the azimuth angle of the reflector. The axis of the horizontal axis is parallel to the ground, which can control the elevation angle of the reflector. The height from the intersection of two rotating axes (also known as the center of the heliostat) to the ground is called the installation height of the heliostat. A tower power station utilizes a large number of heliostats to form an array, known as a heliostat field ^[2]. The heliostat concentrates the reflection of sunlight onto a collector installed at the top of the absorption tower in the mirror field, heats the thermal conductive medium inside, and stores solar energy in the form of thermal energy, which is then converted from thermal energy to electrical energy through heat exchange. Sunlight is not a parallel beam of light, but a beam of conical light with a certain conical angle, so the reflected light from the sun at any point of the heliostat is also a beam of conical light. When the heliostat is working, the control system controls the normal direction of the heliostat in real-time based on the position of the sun, so that the light emitted from the center of the sun is reflected by the center of the heliostat and directed towards the center of the collector. The height above the ground of the center of the collector is called the height of the absorption tower. We plan to build a circular heliostat field in a circular area located at 98.5°E, 39.4°N, with an elevation of 3000m and a radius of 350m. The mirror field coordinate system is established by taking the center of the circular area as the origin, with the east direction being the positive direction of the x axis, the north direction being the positive direction of the y axis, and the upward direction perpendicular to the ground being the positive direction of the z-axis.

The planned height of the absorption tower is 80m, and the collector adopts a cylindrical external light collector with a height of 8m and a diameter of 7m. There is no heliostat installed within 100 meters around the absorption tower, and an open space is left for the construction of a factory building for the installation of equipment such as power generation, energy storage [3], and control. The shape of a heliostat is a flat rectangle, with its upper and lower edges always parallel to the ground. The distance between these two edges is called the mirror height, and the distance between the left and right sides of the mirror is called the mirror width. Usually, the mirror width is not less than the mirror height. The length of the mirror surface is between 2m and 8m, and the installation height is between 2m and 6m. The installation height must ensure that the mirror surface does not touch the ground when rotating around the horizontal axis. Due to the need for maintenance and cleaning of vehicles, it is required that the distance between the centers of adjacent heliostat bases be more than 5m wider than the width of the mirror surface.

If the absorption tower is built at the center of the circular heliostat field, the size of the heliostat is all 6m × 6m, with an installation height of 4m, and given the positions of all heliostat centers, calculate the annual average optical efficiency, annual average output thermal power, and annual average output thermal power per unit mirror area of the heliostat field. According to the design requirements, the rated annual average output thermal power (hereinafter referred to as the rated power) of the heliostat field is 60MW [4]. If all heliostats have the same size and installation height, this article will design the following parameters for the heliostat field: position coordinates of the absorption tower, heliostat size, installation height, number of heliostats, and heliostat position, so that the average annual output thermal power per unit mirror area of the heliostat field is as large as possible under the condition of reaching the rated power. And calculate the position coordinates, heliostat size, installation height, and position coordinates of the absorption tower.

2. Analysis of fixed day field

2.1 Given formula

Firstly, this article calculates the formula for the solar altitude angle α_s and solar declination angle δ based on the given formula:

$$\sin \delta = \sin \frac{2\pi D}{365} \sin \left(\frac{2\pi}{360} 23.45 \right) \quad (1)$$

D is the number of days starting from day 0 based on the vernal equinox, and the number of days D for each corresponding calculation time point is determined based on the date of the vernal equinox.

$$\omega = \frac{\pi}{12} (ST - 12) \quad (2)$$

ω is the solar time angle, where ST is the local time.

The Formula for Calculating the Sun Azimuth Angle γ_s

$$\cos \gamma_s = \frac{\sin \delta - \sin \alpha_s \sin \varphi}{\cos \alpha_s \cos \varphi} \quad (3)$$

By substituting the known parameters into the above formula, the solar altitude angle and solar time angle can be solved.

The normal direct radiation irradiance DNI is

$$DNI = G_0 \left[a + b \exp \left(-\frac{c}{\sin \alpha_s} \right) \right] \quad (4)$$

$$a = 0.4237 - 0.00821(6 - H)^2 \quad (5)$$

$$b = 0.5055 + 0.05595(6.5 - H)^2 \quad (6)$$

$$c = 0.2711 + 0.01858(2.5 - H)^2 \quad (7)$$

Among them, G_0 is the solar constant, with a value of 1.366kW/m². H is the altitude, in this article, H=3000m.

The calculation formula for the output thermal power E of the heliostat field is:

$$E_{field} = DNI \cdot \sum_i^N A_i \eta_i \quad (8)$$

The calculation formula for the optical efficiency of a heliostat is:

$$\eta = \eta_{sb}\eta_{cos}\eta_{at}\eta_{trunc}\eta_{ref} \quad (9)$$

The atmospheric transmittance is:

$$\eta_{at} = 0.99321 - 0.0001176d_{HR} + 1.97 \times 10^{-8} \times d_{HR}^2 \quad (d_{HR} \leq 1000) \quad (10)$$

Distance from the center of the mirror to the center of the collector:

$$d_{HR} = \sqrt{x^2 + Y^2 + H^2} \text{ (unit: m)} \quad (11)$$

The calculation formula for the cutoff efficiency of the collector is:

$$\eta_{trunc} = \frac{\text{Collectors receive energy}}{\text{Specular total reflection energy} - \text{Shadow occlusion loss}} \quad (12)$$

The calculation formula for shadow occlusion efficiency is:

$$\eta_{sb} = 1 - \text{Shadow occlusion loss} \quad (13)$$

The formula for calculating cosine efficiency is:

$$\eta_{cos} = 1 - \text{Cosine loss} \quad (14)$$

Definition of atmospheric quality:

$$AM = \frac{1}{\cos \alpha_s} \quad (15)$$

The formula for irradiance:

$$I_D = 1.3535 \times 0.7^{AM^{0.678}} \quad (16)$$

$$\text{Cosine loss} = \frac{1.353 \times 0.7 - I_D}{1.353 \times 0.7} \quad (17)$$

η_{cos} can be calculated, and the mirror reflectance η_{ref} can be taken as a constant, such as 0.92.

2.2 Calculation of parameters

Firstly, based on the given formula, input the data into Excel for calculation to calculate the solar altitude angle and solar azimuth angle. During the calculation process, some unlikely solar azimuth angles may be encountered, which is a normal situation because the azimuth angle cannot be defined when the sun is overhead. When calculating the optical efficiency of each heliostat, it is necessary to estimate some losses in advance: shadow occlusion loss: because the distance between adjacent heliostats is large enough, this article assumes its losses to be minimal. Cosine loss: Calculate equation (15) based on the definition of atmospheric quality, then formula (16) based on irradiance, and finally calculate equation (17) to obtain η_{cos} .

2.3 Visualization processing

This article visualizes the position of heliostats, as shown in Fig 1. A coordinate system is established with the collector tower as the center, with the east being positive and the north being positive. The position coordinates of each heliostat are marked with blue dots on the coordinate system, indicating that all heliostats are uniformly distributed in a circular area with a radius $r \in (107, 337)$.

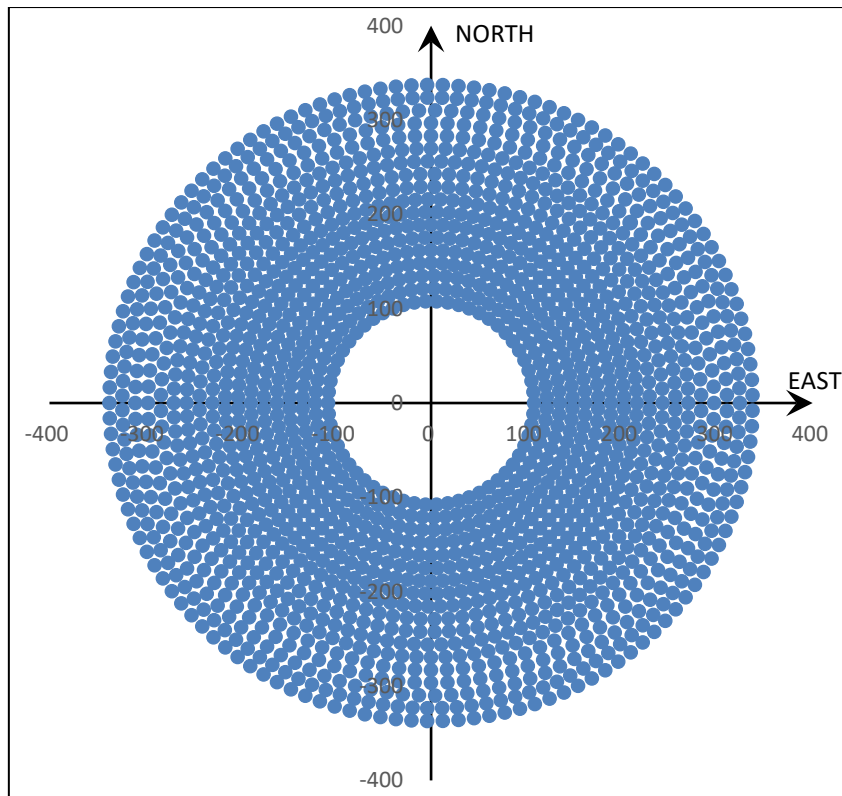


Figure 1: Visualization Coordinate Map of Heliostat

The visualization processing of solar altitude angle and solar azimuth angle is shown in Fig 2, which represents the changes of solar altitude angle and azimuth angle at different times, facilitating the observation of incident angle, reflection angle, etc.

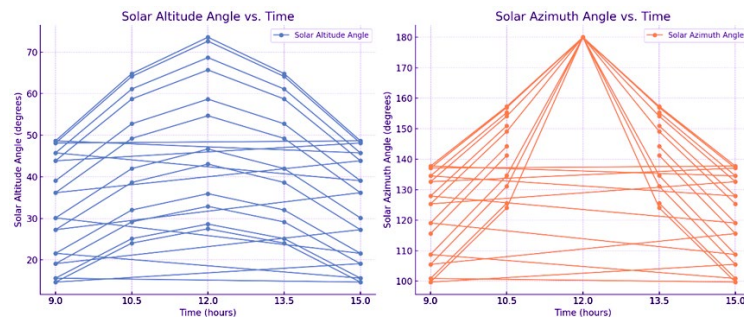


Figure 2: Visualization Data of Sun Azimuth

2.4 Power Calculation

This article has already explained that solar radiation reaches the Earth's surface in the form of a light cone, and provided the size of the light cone. The following further explains the distribution of energy within the light cone. According to the law of reflection, the energy distribution of a solar cone reflected by a heliostat should be the same as the incident solar cone. Therefore, the description can start from the incident light cone. The sun observed from Earth is a circle, commonly referred to as the solar disk. The energy distribution of the solar disk is not uniform but gradually decreases from the inside out. There are many energy models for the solar disk, and here we choose a more common empirical model to describe the energy distribution on the solar disk:

In the formula, S_0 is the energy flow density at a certain point on the solar disk, in W / m^2 ; λ is a constant, with a value of 0.5138; a is the line between any point on the solar disk and an observation point on Earth, which is viewed from the center of the solar disk

The angle between the connecting lines of the measuring points;

$$S_0 = \frac{DNI \cdot dA}{\pi} \quad (18)$$

Based on the above equation, the Monte Carlo method^[5] can be used to obtain the energy flow distribution of the solar disk simulated by the probability distribution of random points, as shown in Fig 3. The specific size of the distribution is determined by the distance between the mirror towers:



Figure 3: Monte Carlo simulation of the distribution of solar cone energy flow density

Similarly, when the heat absorbing surface is at right angles to the central axis^[6] of the light cone reflected by the heliostat, the light spots on the heat absorbing surface will also exhibit the distribution shown in the figure above.

The direction of the sun's rays varies with the position of the sun. For the convenience of future calculations, the coordinate representation of the sun's rays in the mirror field coordinate system is first provided here. To avoid discussing the non parallelism of solar rays, start with the main incident rays R (Rx, Ry, Rz) of the solar cone (i.e. the central axis of the cone). Under the premise that the volume of the sun is 130 times that of the Earth, the sunlight received in the same area can be regarded as parallel light, so the sun's altitude and azimuth can be used to express the sunlight. To facilitate the description of each vertex, a new coordinate system is introduced for each heliostat: the heliostat coordinate system. This article names the two long edges of the heliostat that are always parallel to the ground as L, with a length of l. The other two perpendicular edges are called K, with a length of k. Take the center of the heliostat as the coordinate origin of the heliostat coordinate system; The y-axis is parallel to L when passing through the origin, and the easterly side is positive; The y-axis is parallel to K when passing through the origin, and the north side is positive; Passing through the origin perpendicular to the mirror is the z-axis, and pointing towards the zenith is positive.

3. Model solving

3.1 Calculation of output thermal power

Firstly, perform the solar declination angle δ According to formula (1), calculate the number of days starting from the 0th day using the vernal equinox as the corresponding D, as shown in Table 1 Table 2 and Table 3:

Table 1: Relationship between Date, Days, and Sine Value of the Sun's Declination Angle

date	Days	Sine formula of solar declination angle
January 21st	D=306	$\sin \delta=0.000656$
February 21st	D=337	$\sin \delta=0.000722$
March 21st	D=0	$\sin \delta=0$
April 21st	D=31	$\sin \delta=0.000067$
May 21st	D=61	$\sin \delta=0.000131$
June 21st	D=92	$\sin \delta=0.000197$
July 21st	D=122	$\sin \delta=0.000262$
August 21st	D=153	$\sin \delta=0.000328$
September 21st	D=184	$\sin \delta=0.000395$
October 21st	D=214	$\sin \delta=0.000459$
November 21st	D=245	$\sin \delta=0.000525$
December 21st	D=275	$\sin \delta=0.000590$

The calculation of solar time angle is based on formula (2)

Table 2: Relationship between local time and solar time angle

local time	Solar hour angle
ST1=9	$\omega_1=-0.785$
ST2=10.5	$\omega_2=-0.393$
ST3=12	$\omega_3=0$
ST4=13.5	$\omega_4=0.393$
ST5=15	$\omega_5=0.785$

The calculation of normal direct radiation irradiance DNI is based on formulas (4-7)

Table 3: Monthly Normal Direct Radiation Irradiance and Annual Average Irradiance Table

a		0.34981	
b		0.57839	
c		0.27575	
January	February	March	April
DNI1	DNI2	DNI3	DNI4
0.99780	0.99782	0.99767	0.99768
May	June	July	August
DNI5	DNI6	DNI7	DNI8
0.99769	0.99771	0.99772	0.99774
September	October	November	December
DNI9	DNI10	DNI11	DNI12
0.99775	0.99776	0.99778	0.99779
Annual average normal direct radiation irradiance			
\overline{DNI}			
0.99774			

3.2 Modeling the reflection characteristics of heliostats

In order to better understand the reflection effect of sunlight on the mirror surface of a heliostat, this article establishes an interaction model^[7] between sunlight and the heliostat, which can more intuitively observe the interaction between the two and determine a heliostat size and material that maximizes the reflection of sunlight. Due to the fact that sunlight is a conical light with a certain cone angle, this article uses the formula

$$\vec{d} = \begin{bmatrix} \sin(\theta) & \cos(\varphi) \\ \sin(\theta) & \sin(\varphi) \\ & \cos(\theta) \end{bmatrix} \quad (19)$$

To describe the direction of sunlight. Among θ is the angle between sunlight and the vertical direction, φ The direction of sunlight on a horizontal plane. The reflected light \vec{r} can be calculated according to the formula:

$$\vec{r} = \vec{d} - 2(\vec{d} \cdot \vec{n})\vec{n} \quad (20)$$

Calculate and obtain, where $(\vec{d} \cdot \vec{n})$ is the dot product between the direction of sunlight and the normal vector. In order to make the model more practical, this article needs to know the position of the sun at a specific time and location in order to obtain the sun's altitude angle and azimuth angle. After obtaining the position of the sun, it is necessary to determine the direction of the heliostat in order to calculate the direction of reflected light. After obtaining the above results, subsequent calculations can be carried out to calculate the output thermal power of the heliostat based on the model.

Fix the position of the absorption tower^[8] at the center of the mirror field and set the size of the heliostat to 6m×6m. Optimize the position and quantity of heliostats to maximize the annual average output thermal power per unit mirror area. The initial number of fake heliostats is 1000, and the fitness function will calculate the annual average output thermal power per unit mirror area based on the position of heliostats, the number of heliostats, and the position of the sun. In genetic algorithms, each solution represents a possible heliostat configuration, where genes represent the position of the heliostat. Through selection, crossover, and mutation operations, more new solutions can be obtained, gradually approaching the

optimal solution.

3.3 Heliostat field analysis

The heliostat field planning of this study is based on the 6282 mirror field^[9], and the distribution of heliostats in this mirror field is shown in Fig 4.

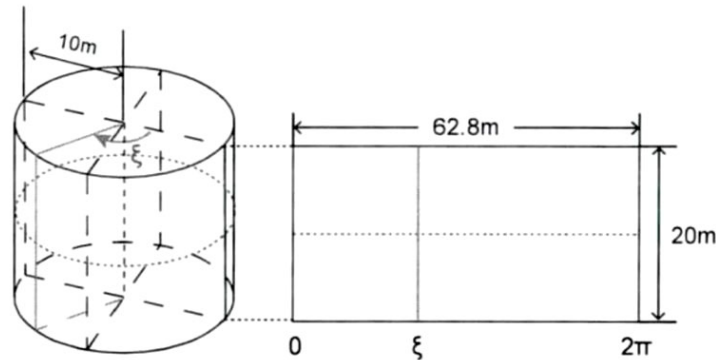


Figure 4: Distribution of heliostats in the mirror field

Among them, the positive directions of the x-axis and z-axis point to due east and south, respectively, while the y-axis points to the sky. The heliostat field consists of 6282 heliostats, which are distributed in a circular pattern around the receiver, leaving a channel directly south of the receiver. In practical scenarios, it is convenient for workers to enter the field for repair, debugging, and other work^[10]. Due to the location of the mirror field in the northern hemisphere, sunlight is emitted from the south. In order to increase the radiation energy density received by the receiver surface, the heliostats of the mirror field are more placed in the north. As the distance between the heliostat and the receiver gradually increases, the number of heliostats on the south side gradually decreases. Each heliostat in the mirror field is a rectangle 4 meters long and 3.2 meters wide, with a height of 3 meters from the center of the heliostat to the ground. The outermost radius of the annular heliostat field is 660 meters, and the new field generated in subsequent optimization studies is also bounded by this. The receiver is located in the center of the heliostat field and is a cylindrical shape with a height of 20 meters and a radius of 10 meters, with a height of 180 meters from the ground. The final radiation energy simulation results can be obtained by unfolding the surface of the cylindrical receiver along the axis^[11]. Due to the gap in the field of the due south heliostat, this article stipulates that the receiver should be unfolded clockwise along the due south axis.

4. Conclusions

This article calculates the average optical efficiency, average cosine efficiency, average shadow occlusion efficiency, average truncation efficiency, and average output thermal power per unit area mirror at different time periods each month by calculating the solar altitude angle, azimuth angle, normal direct radiation irradiance, output thermal power, and optical efficiency. To analyze the maximum efficiency achievable by the heliostat model in different months and periods, and further analyze the improvement of solar power generation efficiency.

The advantages of this article's modeling are easy to understand and calculate, low computational complexity, fast running speed, strong interpretability, simple implementation, and low storage resources required. However, the algorithm used in the model applied in this article is relatively lacking, and the results have strong specificity, making it difficult to apply to more practical problems related to life.

By optimizing the design of the heliostat field, this study has achieved significant results in the selection of mirror materials, structural design, and optical performance optimization. Experiments have shown that the optimized heliostat field has a significant improvement in focusing efficiency compared to traditional design, and has good engineering application prospects, which has positive significance for the development of solar energy technology.

References

- [1] Liu Jiaying. *Design of a tower solar heliostat tracking control system* [J]. *Central North University*, 2023 (01).
- [2] Sun Hao, Gao Bo, Liu Jianxing. *Research on the layout of heliostat field in tower solar power plants*. *Power Generation Technology*, 2021, 12 (6).
- [3] K. El Alami, M. Asbik, H. Agalit, *Identification of natural rocks as storage materials in thermal energy storage (TES) system of concentrated solar power (CSP) plants – a review*, *Sol. Energy Mater. Sol. Cells* 217 (Nov. 2020), 110599, <https://doi.org/10.1016/j.solmat.2020.110599>.
- [4] D. Feldman, V. Ramasamy, R. Fu, A. Ramdas, J. Desai, R. Margolis, *U.S. Solar Photovoltaic System And Energy Storage Cost Benchmark: Q1 2020*, Technical Report: NREL/TP-6A20-77324, National Renewable Energy Laboratory (NREL), US Department of Energy, 2021 [Online]. Available: <https://www.nrel.gov/docs/fy21osti/77324.pdf>.
- [5] Zeng Xiangwei, Zhang Yan, Yang Junxiu. *Optimization algorithm for forward propagation in scattering environment based on polarization Monte Carlo method* [J/OL]. *Journal of Optics: 1-14*[2023-10-23]. <http://kns.cnki.net/kcms/detail/31.1252.O4.20230207.1634.047.html>.
- [6] Speetzen, N., Richter, P., 2021. *Dynamic aiming strategy for central receiver systems*. *Renew. Energy* 180, 55–67. J. Yellowhair, P.A. Apostolopoulos, D.E. Small, D. Novick, M. Mann, *Development of an aerial imaging system for heliostat canting assessments*, *AIP Conf. Proc.* 2445 (May 2022) (2022)
- [7] Marie Pascaline Sarr, Ababacar Thiam, Biram Dieng. *ANFIS and ANN models to predict heliostat tracking errors*[J]. *Heliyon*, 2023(01)
- [8] R.A. Mitchell, G. Zhu, *A non-intrusive optical (NIO) approach to characterize heliostats in utility-scale power tower plants: Methodology and in-situ validation*, *Sol. Energy* 209 (July) (2020) 431–445, <http://dx.doi.org/10.1016/j.solener.2020.09.004>.
- [9] S. Bai, et al., *Dolomite-derived composites doped with binary ions for direct solar thermal conversion and stabilized thermochemical energy storage*, *Sol. Energy Mater. Sol. Cells* 239 (2022), 111659.
- [10] S. Bai, et al., *Structurally improved, TiO₂-incorporated, CaO-based pellets for thermochemical energy storage in concentrated solar power plants*, *Sol. Energy Mater. Sol. Cells* 226 (2021), 111076.
- [11] Murphy C, Sun Y, Cole W, Maclaurin G, Turchi C, Mehos M. *The potential role of concentrating solar power within the context of DOE's 2030 solar cost target*, Golden, CO: National Renewable Energy Laboratory; 2019. NREL/TP-6A20-71912 www.nrel.gov/docs/fy19osti/71912.pdf visited July 2, 2020.